

Mineral Resources Tasmania

ASTER Processing and Interpretation of Northeast Tasmania

May 2007

Compiled by:

Endorsed by:

Daryl Nunn
Consultant Name
Daryl Nunn

Stephen Nano
Principal Name
Stephen Nano

Authors: Marty Moloney, Daryl Nunn & Stephen Nano

Our Ref: JN1077

Table of Contents

1. EXECUTIVE SUMMARY	3
2. INTRODUCTION	5
3. ASTER SENSOR.....	5
4. ASTER SCENE SELECTION.....	6
5. ASTER IMAGE PROCESSING	7
5.1. PRE-PROCESSING.....	7
5.1.1. VNIR/SWIR Spectral Corrections - Crosstalk and Atmospheric	7
5.1.2. TIR Spectral Corrections – Atmospheric and Emissivity	7
5.1.3. Rectification	7
5.2. FALSE COLOUR IMAGE MOSAICING	7
5.3. MINERAL MAPPING	8
5.3.1. SWIR Mineral Mapping.....	8
5.3.1.1. Selecting Local Spectra	8
5.3.1.2. SWIR Mineral Distribution Maps	9
5.3.1.3. SWIR Mineral Abundance Maps	10
5.3.2. VNIR Mineral Mapping (Fe-oxide Distribution Maps)	10
5.3.3. TIR Mineral Mapping (Silica Abundance Maps)	10
6. RESULTS OF ASTER PROCESSING	10
6.1. FALSE COLOUR IMAGES	10
6.2. MINERAL MAPPING	10
6.2.1. Distribution/Intensity Maps	10
6.2.2. Mineral Intensity Maps.....	11
7. INTERPRETATION	11
8. RESULTS OF INTERPRETATION.....	12
9. DISCUSSION.....	13
TIN-TUNGSTEN MINERALISATION IN NORTH EASTERN TASMANIA	14
Endogranitoid tin deposits.....	14
Exogranitoid tin deposits.....	14
GOLD MINERALISATION IN NORTH EASTERN TASMANIA	14
ASTER RESPONSES IN ALTERATION CLUSTERS.....	15
Beaconsfield (Alteration Cluster 1).....	15
Lillydale (Alteration Cluster 2)	15
Mathinna (Alteration Cluster 3)	15
Mt Cameron (Alteration Cluster 4)	16
Whitemark (Alteration Cluster 5)	16
10. REFERENCES	17
11. DVD DATA REFERENCE LIST	18



1. Executive Summary

Global Ore Discovery was commissioned by Geoff Green of the Mineral Resources of Tasmania to undertake a program of ASTER image processing, mineral mapping and alteration interpretation over northeast Tasmania. The investigation was conducted to characterising the ASTER spectral response over known mineral deposits and to map the distribution of other alteration systems, visible to the Aster sensor, that maybe indicators of under / unexplored mineralized systems.

Eight (8) ASTER scenes were selected, atmospherically corrected, and three false colour images mosaics and a greyscale image base were created to aid in interpretation.

- TM741Sim
- SWIR468
- VNIR231

A proprietary mineral mapping procedure was applied to corrected data to map the distribution of minerals to which ASTER is “sensitive”. Mineral Distribution Maps were thereby created which show areas where there is a high probability of finding the following minerals:

- Kaolinite
- Muscovite (sericite)
- Pyrophyllite
- Alunite
- Chlorite/epidote
- Silica
- Fe-oxide

Mineral Abundance Maps were then created which highlight the variation of the mineral mapping response (i.e. the variation in abundance) within the areas contained by selected groups of Mineral Distribution Maps. These groups comprise:

- Acid Sulphate (Pyrophyllite + Alunite)
- AIOH (Kaolinite + Sericite)
- Propylitic (Chlorite/Epidote)
- Silica

These mineral maps were the interpreted with the aid of ASTER false colour images and geological information with the aim of removing false responses due to lithology, cloud, water etc. The resulting interpretative layer provides a simplified version of the mineral mapping results that is suitable for geological analysis.

Six (6) broad alteration clusters have been identified in this interpretative layer however, other more isolated responses exist throughout the study area and might be equally significant.

In these clusters the following observation have been made

- A well zoned alteration pattern is exhibited by the ASTER responses that comprise the Whitemark target on Flinders Island where several alluvial tin prospects were explored in the 1950s and 60s. Little modern exploration data has been found to describe the primary mineralisation style(s) in this area.
- Some Exogranitoid deposits have silica/kaolinite/muscovite signatures. An arcuate zone of Fe-oxide, AIOH & silica ASTER anomalies extending from 4 km south to 14 km east of Pioneer warrants follow-up for Exogranitoid-type mineralization.
- Silica, Fe-oxide, kaolinite and other minerals have been mapped in the Beaconsfield district and in the surrounding region
- Along a corridor in the Dans Rivulet, Mathinna and Tower Hill districts Fe-oxide, alunite & silica dominated ASTER responses are noted.
- Several ASTER responses occur where no mineral occurrences are known.

There are a number of known mineral occurrence and or belts that have not returned responses detectable by ASTER. In general this could be due to a range of factors including;



- Alteration minerals are unable to be detected by the ASTER sensor
- The alteration halos maybe volumetrically too small to be resolved with the spatial resolution of the ASTER sensor.
- Vegetation masking of the alteration response.
- Post mineral cover including shallow soil and alluvium

In this study it is likely that the dominant effects on responses are the widespread dense vegetation cover and the post-Carboniferous cover sequences over the mineralized and often recessive Ordovician-Devonian rocks in many areas e.g. above the intrusion-related gold deposits of the Lisle area (Callaghan, 2004).

It should be stressed that the analysis approach adopted in this study aimed to derive alteration-related ASTER anomalies from the detection of strong ("deep") absorption features by comparing all spectra in each image area. In following-up the results of this investigation workers should consider an alternative approach whereby ASTER data analysis is conducted at the mining-camp scale in order to detect and characterize more subtle spectral variations.

The results presented in this report should be incorporated into an integrated targeting exercise that includes a geochemical, geophysical & structural/stratigraphic synthesis for the purpose of prioritising the alteration anomalies presented on Map 1, and for planning follow-up field programmes.

2. Introduction

Global Ore Discovery (Global Ore) has undertaken processing and interpretation of ASTER imagery over north-eastern Tasmania on behalf of Mineral Resources Tasmania (MRT). This region hosts a number of known intrusive related and orogenic Au deposits as well as granitoid related Sn-W mineralisation. Processing and interpretation of ASTER imagery was undertaken to ‘fingerprint’ the spectral response of the known deposits and to highlight additional areas of hydrothermal alteration that may host mineralisation.

This report details the processing and interpretation undertaken by Global Ore, and describes the products supplied to MRT.

3. ASTER Sensor

In December 1999, a joint effort between NASA and Japans Ministry of International Trade and Industry (MITI) launched the Advanced Space borne Thermal Emission and Reflection Radiometer (ASTER) on board NASA’s Terra spacecraft. Acquiring reflectance data from the visible to the thermal infrared at moderate spatial, spectral and radiometric resolution, ASTER provides earth scientists with an excellent data source to map surface materials on the Earth. Three modules at varying spatial and spectral resolutions collect the ASTER data (Table 1). Each ASTER scene covers an area of approximately 60 x 60 km (Landsat TM covers about 180 x 180 km).

ASTER’s improved spectral resolution, over Landsat TM (Figure 1), within the short wave (SWIR) and thermal infrared (TIR), allows the mapping of a select range mineral species within the sulphate, carbonate, layer silicate, silicate and Fe-oxide mineral groups. This gives exploration geologists a previously unavailable opportunity to map mineral zonation within hydrothermal systems over large areas of the Earth at minimal cost.

Table 1. Spectral and spatial characteristics of the three ASTER instruments

Characteristic	VNIR Module	SWIR Module	TIR Module
Spectral Range	Band 1: 0.52 - 0.60 μm Band 2: 0.63 - 0.69 μm Band 3: 0.76 - 0.86 μm Band 3: 0.76 - 0.86 μm Backward looking Band	Band 4: 1.600 – 1.700 μm Band 5: 2.145 – 2.185 μm Band 6: 2.185 – 2.225 μm Band 7: 2.235 - 2.285 μm Band 8: 2.295 - 2.365 μm Band 9: 2.360 - 2.430 μm	Band 10: 8.125 - 8.475 μm Band 11: 8.475 - 8.825 μm Band 12: 8.925 - 9.275 μm Band 13: 10.25 - 10.95 μm Band 14: 10.95 - 11.65 μm
Ground Resolution	15 m	30m	90m
Swath Width (km)	60	60	60

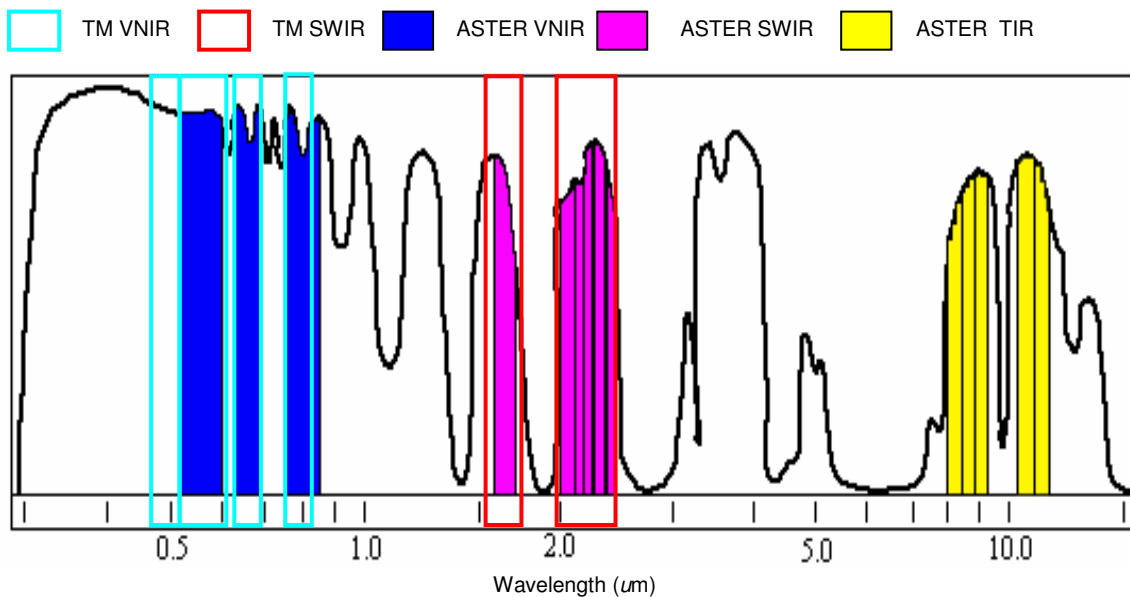


Figure 1. Comparison between the spectral characteristics the ASTER and Landsat TM satellites. ASTER provides six (6) bands in the SWIR vs Landsat’s two (2). ASTER also provides a five (5) bands in the TIR where Landsat TM has none.

4. ASTER Scene Selection

Eight ASTER scenes were selected from the ASTER scene library for the purposes of this investigation. The ASTER processing was to be undertaken over the full area of each of these scenes (Figure 2).

Preference was given to images acquired on the same day (known as scene “runs”), which gives virtually identical atmospheric conditions over those scenes. This is ideal for providing a consistent basis for mineral mapping. The selection of scenes also considered distribution of cloud-cover. Where possible, scenes were selected from the local dry season such that the effect of vegetation could be reduced.

The selected scenes have the characteristics as described in Table 2. A “Short ID” was attributed to each selected scene to facilitate file-level data management during processing. Two runs were available, collected on the 13th July, and 22nd July 2006. Cloud cover exists in some of the scenes, thus additional scenes were selected with significant amount of overlap to provide a near complete cloud free coverage of the original area of interest.

Table 2. Characteristics of ASTER scenes.

ASTER L1A ID	Short ID	Date	Cloud Cover
SC:AST_L1A.003:2006229335	AST270	29 Mar 2000	0
SC:AST_L1A.003:2035100842	AST271	13 Jul 2006	0
SC:AST_L1A.003:2035100864	AST272	13 Jul 2006	0
SC:AST_L1A.003:2035100900	AST273	13 Jul 2006	0
SC:AST_L1A.003:2027188630	AST274	30 Dec 2004	0
SC:AST_L1A.003:2033732457	AST275	01 Apr 2006	8
SC:AST_L1A.003:2035295233	AST276	22 Jul 2006	19
SC:AST_L1A.003:2035295235	AST277	22 Jul 2006	7

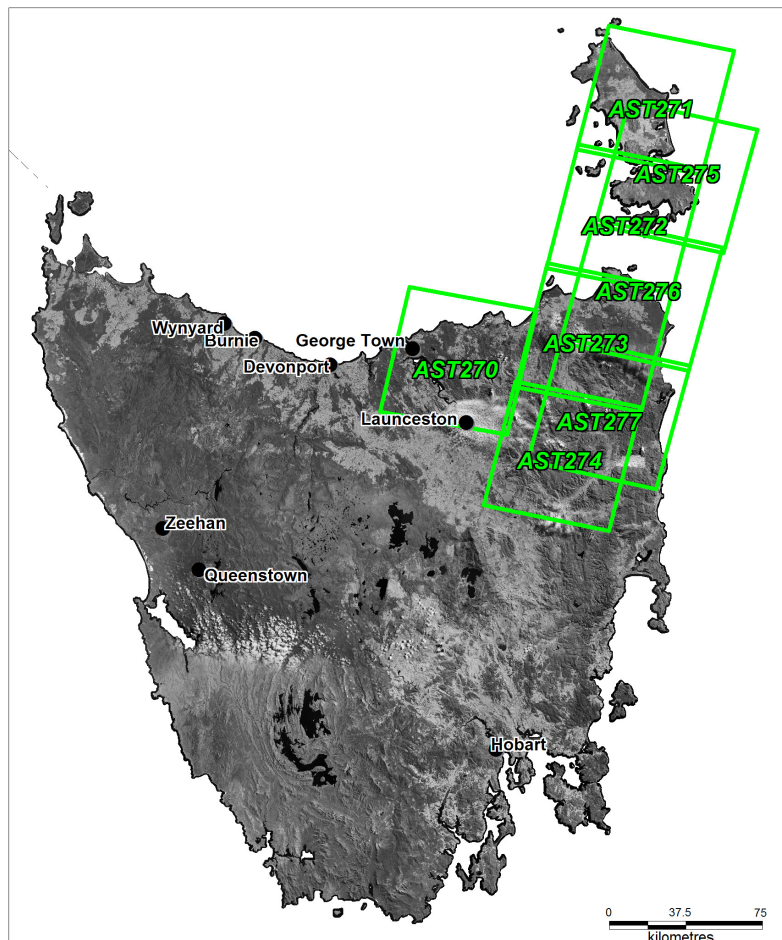


Figure 2. MRT Landsat TM 741 mosaic showing individual ASTER scene boundaries used in this investigation.

5. ASTER Image Processing

The ASTER image processing was conducted using ENVI and ERMapper software in three (3) basic stages;

- *Pre-processing.* The ASTER images were corrected for atmospheric and other spectral effects, and then registered to MRT's Landsat TM base.
- *False Colour Image Mosaicing.* Three (3) false colour image mosaics were then created. These images provide important qualitative control for the interpretation process.
- *Mineral Mapping.* A series of spectral analysis methods were applied resulting in a suite "mineral maps". Mineral maps are essentially probability maps that indicate likely occurrences of the suite of target minerals that are often associated with hydrothermal alteration.

These processing stages are further explained below...

5.1. Pre-processing

5.1.1. VNIR/SWIR Spectral Corrections - Crosstalk and Atmospheric

The following steps were undertaken for each ASTER image;

1. The crosstalk correction was applied to the SWIR bands of each ASTER image. Spectral crosstalk is a phenomenon whereby diffuse incident light from band 4 is reflected onto other bands from the metal film at the back of each detector. The diffused image of band 4 is subtracted from the images of the other bands using software supplied by the ASTER GDS (ASTER Science Project Website, 2007)
2. The VNIR and SWIR bands were "stacked" into a single file at 30m resolution. This stacked file was then atmospherically corrected using the FLAASH plug-in for ENVI.
3. A subset containing only VNIR bands at 15m was created, and also atmospherically corrected using FLAASH.

5.1.2. TIR Spectral Corrections – Atmospheric and Emissivity

The TIR bands were processed to remove the atmospheric effect and derive emissivity values.

ENVI's "Thermal Atm Correction" utility was used to approximate and remove the atmospheric contributions to the ASTER TIR data. This atmospheric correction algorithm used in ENVI is similar to the In-Scene Atmospheric Compensation algorithm, proposed by Johnson and Young (1998).

5.1.3. Rectification

MRT has provided a Landsat image mosaic for the purpose of establishing a consistent spatial control between the various ASTER images. Each ASTER scene was rectified to the MRT Landsat image mosaic such that any displacement was minimised to approximately 30-50m.

5.2. False Colour Image Mosaicing

A set of false-colour image mosaics were then produced for the ASTER scenes (see 6.1). The individual images were mosaiced and colour-balanced to produce a single image for each false-colour stretch. The mosaiced images comprise:

- *A 231 stretch.* This image uses data exclusively from ASTER's visual and near-infrared (VNIR) sensor, and therefore has the highest resolution (15m) of the image suite. This image is a pseudo-true colour image, with green representing vegetation, and shades of white-brown-black representing similar lithological variations that the eye would perceive.
- *A 468 stretch.* This image uses ASTER's shortwave-infrared (SWIR) sensor, which has a 30m resolution. These bands are highly sensitive to lithological and alteration variations and are in a



region of the electromagnetic spectrum that the eye cannot perceive. This is therefore the recommended image for geological/alteration interpretation.

- *A TM 741 simulation.* This images uses both the SWIR and VNIR to produce an emulation of the of the classic Landsat Thematic Mapper “741” stretch, which combines high-resolution VNIR data with SWIR geologic information.
- *A Greyscale image.* This image is a greyscale version of the TM 741 simulation product.

These images have been provided in MapInfo format using ecw compression.

5.3. Mineral Mapping

Mineral mapping is a statistical process of identifying areas (image pixels) where there is a high probability of there occurring selected target minerals. The minerals targeted in this investigation comprise muscovite, kaolinite, alunite, pyrophyllite, chlorite, epidote, silica and iron-oxide.

A number of statistical approaches are used in mineral mapping. These approaches are different for each of the three ASTER instruments (VNIR, SWIR & TIR). These three instruments provide data at three resolutions (15m, 30m & 90m respectively). The mineral mapping is therefore conducted in three separate stages with results being provided at these respective resolutions.

5.3.1. SWIR Mineral Mapping

The ASTER SWIR instrument provides data with excellent spectral characteristics (resolution & signal to noise) which allows for the identification of a number of important mineral species. These mineral species become “targets” of the mineral mapping process as applied to any particular instrument. For this investigation the SWIR target mineral species comprise muscovite, kaolinite, epidote, chlorite, alunite and pyrophyllite.

Because there are a relatively large number of SWIR targets of interest to this investigation, and because those targets represent minerals of great significance in alteration studies, we provide a two-fold analysis of the ASTER’s SWIR data that includes quantitative information on both the distribution and abundance of the target mineral species. In this respect, a set of Mineral Distribution Maps provide a measure of where it is likely to find a given mineral species. Mineral Abundance Maps are designed to provide a measure of the intensity (moderate or strong) of selected *combinations* of Distribution Maps.

5.3.1.1. Selecting Local Spectra

Global Ore Discovery has developed a proprietary methodology for deriving Mineral Maps from the ASTER SWIR instrument. Fundamental to this methodology is a spectral library that is composed of spectra from ASTER imagery over “type” localities worldwide. The ASTER imagery in these localities displays excellent and clear responses (spectra) that, with a high degree of certainty, can be attributed the minerals targeted for this investigation. However, because of the varying interference factors, such as atmospheric conditions and vegetative cover, which inherently vary between such diverse ASTER scenes, these type spectra are not used to directly in the Mineral Mapping process.

Rather, the individual spectra from the type library were used to derive a similar *set* of libraries composed of spectra from the ASTER scenes being investigated. These new libraries contain *local* spectra which have characteristic spectral shapes and absorption “depths” similar to the type library. Where a scene formed part of a run, the best spectra from the entire run were selected. The subsequent mineral mapping would then use a *unique spectral library for each collection day* of the ASTER scenes being analysed. Thus five (5) spectral libraries were created for this investigation. Figure 3 illustrates the typical spectra of the SWIR target minerals as derived from the ASTER scenes used in this investigation.

This process of spectra selection is a manual and somewhat subjective process, albeit assisted by a number of statistical methods (e.g. band ratios). Other methods (e.g. PPI/n-D visualisation) allow for an almost fully automated selection of scene spectra to be performed from any given ASTER scene. However, the more manual process provides the analyst an understanding for the spectral variability within the data from inspecting hundreds of individual spectra – this provides a basis from which to assess the results of the subsequent mineral mapping.



SWIR mineral mapping is then a process of identifying target minerals throughout the ASTER imagery using the library spectra. This process is based on the assumption that, for areas where the target mineral can be effectively observed by the sensor, the resulting ASTER spectra will approximate those in the library. Since the *local* library and image spectra are subject to identical atmospheric conditions then we can ascribe a greater level of confidence to this assumption than if we had simply used the type library.

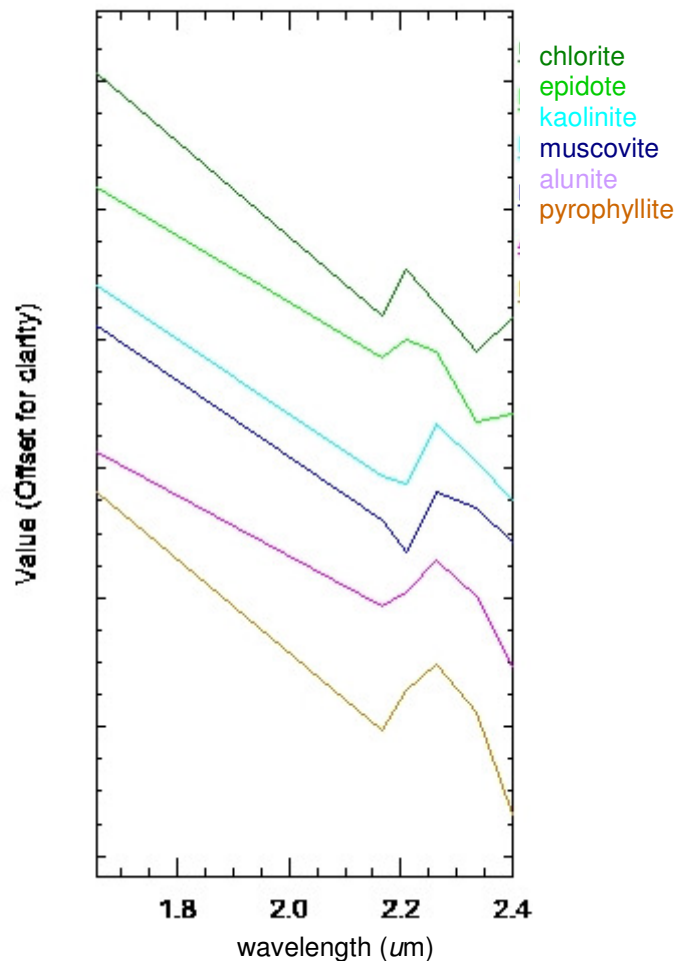


Figure 3. Typical local ASTER spectra used for SWIR mineral mapping in this investigation. These six spectra have been presented in both normal (left, y-axis represents *reflectance*),

Even localities were the ASTER response of a given mineral may be more subtle due to mixing, vegetative cover etc, can be identified by the methods used.

5.3.1.2. SWIR Mineral Distribution Maps

The SWIR library spectra were used in a modified Mixture Tuned Match Filter (MTMF) mineral mapping processing procedure which results in two (2) probability values / ASTER pixel / library spectra (Boardman, 1998). The two MTMF values are referred to as a “score” (a measure of abundance), and an “infeasibility” (a secondary measure of the closeness of fit between the spectra of an image pixel and the library spectra).

Most false-positive anomalies can be avoided by simultaneously inspecting the MTMF infeasibility and score values using a scatter-plot. The Mineral Distribution Map is created by applying a 2-dimensional selection (or threshold) to these parameters (pixels with high threshold and low infeasibility are selected for the Map). The 2-D selection is varied and interactively compared with the geographical distribution of the selected pixels. The final selection is based on the analyst’s assessment of this distribution and is assisted by ancillary data of known or likely alteration/lithological occurrences of the target mineral, and the nature of the spectra within the threshold areas.

The gridded images were then converted to vector layers for use in the GIS, and thus there is a corresponding “Mineral Distribution Map” for each of the target mineral species.

5.3.1.3. SWIR Mineral Abundance Maps

The Mineral Distribution Maps were then used to produce a set of Mineral Abundance Maps.

Three (3) categories of absorption features are considered in this process, the AIOH absorption, an “Acid Sulphate” absorption, and a “Propylitic” absorption. For each of these categories, two Distribution Maps contribute a measure of “abundance” calculated by the MTMF procedure. Table 2 identifies the relationship between Abundance Maps and the contributing Distribution Maps.

Table 2. Relationship between Abundance Map categories and their contributing Mineral Maps

Abundance Map Category	Contributing Distribution Maps
AIOH	kaolinite, muscovite
Acid Sulphate	alunite, pyrophyllite
Propylitic	epidote, chlorite

The Abundance Maps are created by combining (summing) the MTMF “score” (pseudo abundance) results for each of these Distribution Map combinations. The result is then subset into strong and moderate responses where the strong responses represent approximately the top 10% of combined scores and therefore represent the highest concentration of a mineral group in the scene area.

5.3.2. VNIR Mineral Mapping (Fe-oxide Distribution Maps)

The ferric oxide (f=Fe-oxide) mineral map was produced by using a ratio of band 1 / band 2 of the VNIR instrument (Kalinowski & Oliver, 2004). A vegetation mask, derived from a standard Normalized Difference Vegetation Index (NDVI - Earth Observatory Website, 2007) was applied to the results of this ratio. A high-threshold (i.e. high Fe-oxide) was subsequently applied to create the Fe-oxide Mineral Map, and the results converted to a vector layer for use in the GIS.

5.3.3. TIR Mineral Mapping (Silica Abundance Maps)

The silica mineral maps were derived from an algorithm (MMAJ, 2000) that provides an approximation of total SiO₂ content. Two thresholds were applied to the results of this algorithm in order to identify moderate (65%) and strong (71%) silica.

These thresholds then combined into a single vector layer for use in the GIS.

6. Results of ASTER Processing

The processing results are presented as a series of MapInfo tables, explained below. Each filename provided as part of this investigation has a “NETAS_” prefix.

6.1. False Colour Images

‘NETas_ASTER_231RGB_Mosaic.tab’ → Bands 231 in RGB mosaic
 ‘NETas_ASTER_468RGB_Mosaic.tab’ → Bands 468 in RGB mosaic
 ‘NETas_TM741Sim_RGB_Image.tab’ → Landsat 741 Simulation mosaic
 ‘NETas_ASTER_Greyscale_Mosaic.tab’ → Greyscale Image

6.2. Mineral Mapping

6.2.1. Distribution/Intensity Maps

The SWIR distribution map is a single file that maps the distribution of kaolinite, muscovite, chlorite/epidote, pyrophyllite and alunite. The VNIR and TIR Distribution Map filename suffixes denote the particular mineral being mapped.

- NETAS_Combined_SWIR_Dist.tab → Distribution map for kaolinite, muscovite(sericite), alunite, pyrophyllite and chlorite
- NETAS_FeOx_Dist.tab → Fe-oxide distribution
- NETAS_Silica_Dist.tab → Silica Distribution

6.2.2. Mineral Intensity Maps

Two Mineral Intensity Maps are provided, one for the SWIR minerals, and another for silica (derived from the TIR). Each map shows the various Abundance Map Categories (acid sulphate, propylitic, AIOH and silica) at two thresholds; moderate and strong.

- NETAS_Combined_SWIR_Abundance.tab →
- NETAS_Combined_Silica_Abundance.tab →

7. Interpretation

The combined processing results were analysed in conjunction with regional geologic information in order to simplify the range of ASTER image and vector results into three layers (SWIR, Fe-oxide and Silica).

Polygons were digitised where the mineral mapping results were interpreted to represent areas of hydrothermal alteration. These polygons were attributed (see Mapinfo tables) according to the strength and spatial coherency of the mineral mapping results, along with the observed mineral assemblage that characterises the alteration zone. Explanations for the codes used are provided in Table 3.

Table 3. Codes used during the interpretation process.

Strength Code	Explanation	Mineral Code	Explanation
s	strong	c	chlorite
m-s	moderate-strong	e	epidote
m	moderate	k	kaolinite
w	weak	m	muscovite
		p	pyrophyllite
		si	silica
		fe	iron-oxide (ferric)

Note that the mineral assemblage information recorded the relative abundance of minerals that occurred within that interpreted region. The short hand symbology and mineral abbreviations used to attribute the regions is as follows:

- a>b (mineral a has greater abundance than mineral b)
- a-b (mineral a in equal proportions with mineral b)
- a/b (mineral a and or mineral b)

These interpreted polygons represented a wide variety of mineral proportions and combinations. To simplify this information for display and interpretation the polygons have been grouped into mineral assemblage zones that formed under similar pH and temperature conditions. However in some cases it was necessary to group polygons that represent transitional assemblages. These summary groupings can be used to vector within a composite alteration zone and can be used to interpret the temperature and pH conditions of formation and potentially the style of mineralisation (high sulphidation vs low sulphidation epithermal).

In this classification alunite +/- kaolinite represent low temperature (250°C) acid conditions (pH <3.5-4) typical of epithermal advanced argillic conditions. Pyrophyllite is considered to represent low pH (<4.5) conditions moderate temperatures(150-300°C) while and is indicative of transition from advanced argillic to phyllic. Muscovite is considered to be formed at generally higher temperatures (+300°C) than moderate pH (>4.5). However ASTER only has the ability to accurately identify the muscovite group which includes (illite/sericite) which forms at moderate temperatures (150-300°C) and moderate pH conditions (>4.5). In this instance we are suggesting that the response is dominated by muscovite which is indicative of phyllic/greisen assemblages.

The occurrence of propylitic alteration (chlorite/epidote) is considered to represent the outer limits of magmatic systems and is relatively low acid conditions (pH >5.5) and temperatures around 250-300 °C.

The processing technique for silica and Fe-oxides does not discriminate between lithologies that are high in silica or Fe-oxides from hydrothermal derived silica and Fe-oxides. Thus alteration interpretation has focussed on identifying the zones of silica and Fe-oxides associated with hydrothermal minerals interpreted from the SWIR information.

In general a low degree of confidence was ascribed to the alunite and pyrophyllite responses in this interpretive stage. The areas of high abundance of these minerals in the NE Tasmania scenes were generally interpreted to represent pixels where kaolinite might be mixed with vegetation and other surface materials (see Figure 4). In the cases where spectral mixing of kaolinite has been considered the most likely cause of the alunite/pyrophyllite response the “comments” field of the interpretation layer has been attributed to record this.

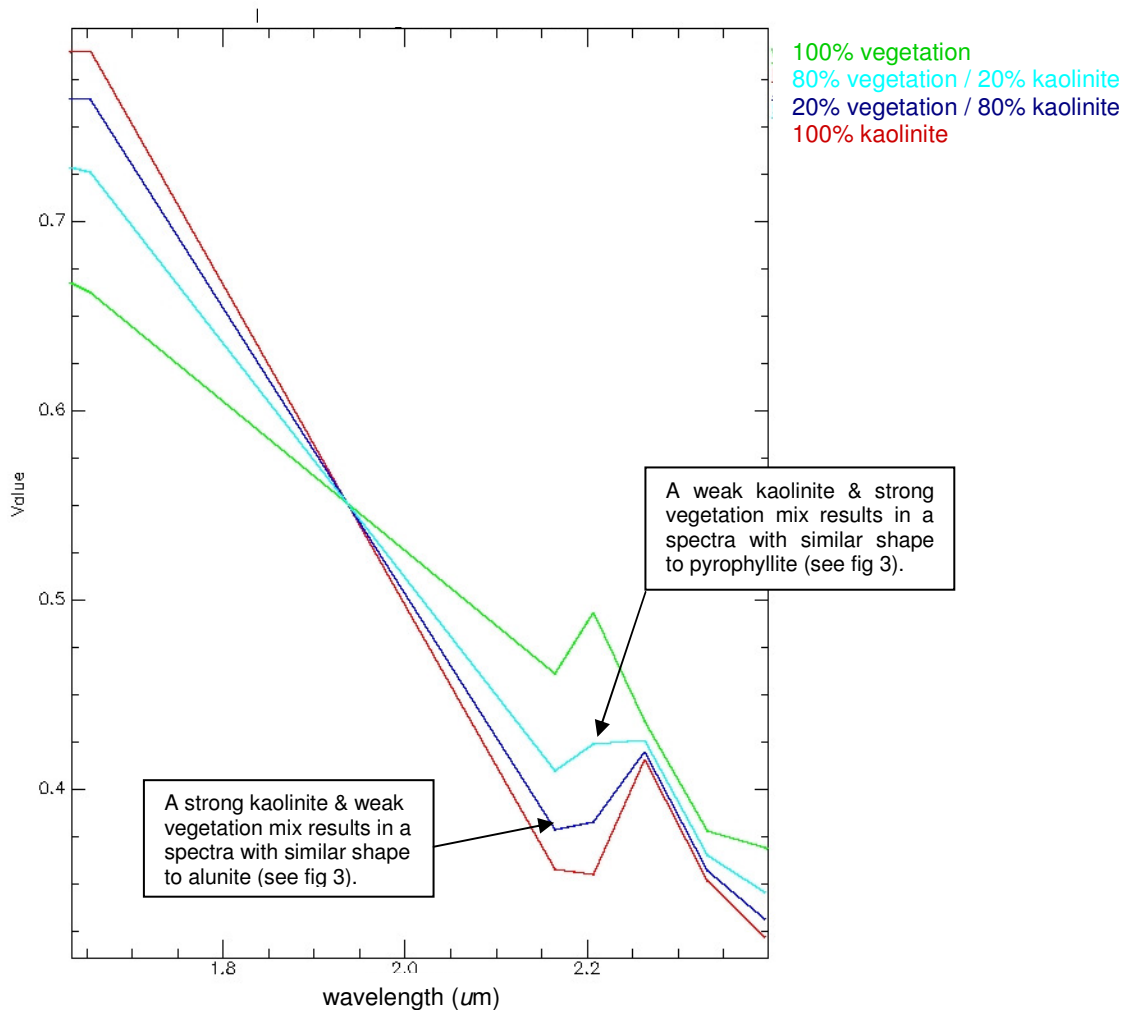


Figure 4. Results of spectral mixing between vegetation cellulose and kaolinite. Note the strong resemblance of the mixed spectra and the local spectra used for mapping pyrophyllite and alunite (see Figure 3).

In some instances the outline of the alteration polygons correlates with the clearings surrounded by dense forest. It is possible that these responses may represent false positives due to the mixing of moderate vegetation with underlying surface materials. However, alternately these may represent de-vegetated widows through to a larger underlying alteration system. This can only be resolved by ground follow-up of this style of responses

8. Results of Interpretation

Three interpretation Mapinfo tables of the VNIR,(Fe-oxide), SWIR(kaolinite etc) and TIR (silica) mineral maps have been generated. In this display of the data solid polygon colours have been used to show the mineral/mineral assemblage that the polygon represents (Figure 5.). Filenames are as follows;

- FeOx_Alteration_Interp.TAB – Fe-oxides alteration polygons
- Silica_Alteration_Interp.TAB –Polygons of interpreted silica alteration
- SWIR_Alteration_Interp.TAB – Interpreted polygons representing areas of alteration evident in the SWIR (kaolinite, muscovite(sericite), alunite, pyrophyllite, chlorite)

This display of the data is useful at large scales and has been used in the production of the area of interest (AOI) overview map presented (Map. 1).

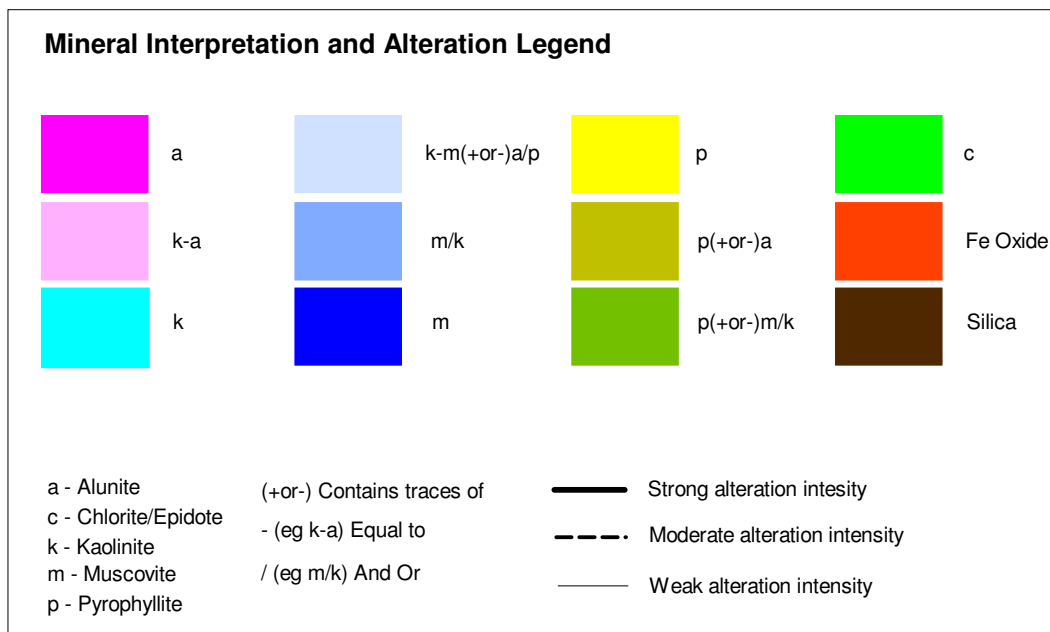


Figure 5. Aster Interpretation legend of polygon colour and lines styles

These three files have been compiled into a single file (NETas_ASTER_Alteration_Interp.TAB) in which the polygons are colour coded to display the mineral/mineral assemblage and line style coded to indicate the intensity/coherency of the response (Figure 5). This display of the data preferred for interpretation but is only applicable at small scales. A series of figures have been produced in areas of interest (Map 2.) using this display style and discussed in Section 9.

9. Discussion

This investigation has identified a number of ASTER alteration responses over known gold & tungsten systems and a number of responses not associated with known mineral occurrences that may represent additional hydrothermal alteration. However, there are a number of known mineral occurrence and or belts that have not returned responses detectable by ASTER. In general this could be due to the a number of factors;

- Alteration minerals are unable to be detected by the ASTER sensor
- The alteration haloes maybe volumetrically too small to be resolved with the spatial resolution of the ASTER sensor.
- Vegetation masking of the alteration response.
- Post mineral cover including shallow soil and alluvium

In this study it is likely that the dominant effects on responses are the widespread dense vegetation cover and the post-Carboniferous cover sequences over the mineralized and often recessive Ordovician-Devonian rocks in many areas e.g. above the intrusion-related gold deposits of the Lisle area (Callaghan, 2004).

As this study incorporates a large area of NE Tasmania the results are herein considered in that context, and one mining camp is compared with another in the discussion below. The results of the ASTER interpretation also appear to fall into several broad clusters, some of which bear a direct relation with the mining camps discussed. These clusters of ASTER responses have divided into the six (6) areas as presented on Map 2.

Detailed AOI ASTER processing, focused on the camp-scale, is warranted to fully assess the spectral response of the individual alteration systems. This would minimise the swamping of statistics which occurs when processing a total scene and allow for the identification of small subtle responses through holes in the canopy or post mineral cover.

Tin-tungsten mineralisation in North Eastern Tasmania

Tin-tungsten mineralization in northeastern Tasmania has yielded about 90,000 t Sn, of which only 65 t was from alluvial deposits. Tungsten production amounts to about 14,000 t WO₃. Primary deposits of include exogranitoid vein systems such as Aberfoyle, Storys Creek & Scamander can possess economic wolframite, cassiterite, molybdenite and bismuthinite mineralisation. Endogranitoid greisens such as Rex Hill & Anchor are usually cassiterite-only lenses and pipes in granites. There are some economic kaolin deposits (e.g. Tonganah) which Taheri & Bottrill (2005) suggest may represent hydrothermally-altered granites.

Endogranitoid tin deposits

The alteration that accompanies the endogranitoid deposits typically results from a geisenisation process whereby feldspars and primary micas have been replaced by topaz and yellow-dark green siderophyllite, with accompanying cassiterite, purple fluorite and apatite. A second stage of hydrothermal alteration has been recognised as a low temperature post-magmatic event during which some topaz and siderophyllite was replaced by sericite, siderite and sulphides. Of the minerals mentioned above, only sericite has a spectral absorption signature that can be mapped with ASTER data, although weathering processes might produce Fe-oxides and clay minerals that ASTER can detect. As the unaltered granites that host the greisens are typically micaceous these deposits are not expected to display the ASTER spectral response which is characteristic of sericite alteration in other deposit styles (a strong AIOH absorption response at 2200 nm). It is not surprising then that no ASTER response is found associated with the low-grade Anchor deposit (0.63 Mt @ 0.49% Sn, located 25 km northwest of St Helens) despite the good exposure of mineralized greisens reported by Taheri & Bottrill (2005).

However, strong ASTER silica and kaolinite responses are seen to be associated with some of these deposits e.g. the Royal George mine, located around 18 km southeast of Avoca. This mine produced 1100 t of Sn in the early 1900s (Ruxton, 1984). CRAE later estimated that 1.2 Mt @ 0.34% Sn remains *in situ* (Purvis, 1981). ASTER silica and kaolinite alteration responses were detected throughout the 5 km zone of tin mineral occurrences that surrounds the Royal George deposit.

Exogranitoid tin deposits

The northeast Tasmanian exogranitoid tin deposits generally occur as sheeted vein systems within the contact metamorphic aureole granitic batholiths. Moderate-strong silica and kaolinite responses are found in the Gladstone area where another contact metamorphic aureole hosts tin and gold mineralisation. However, no ASTER responses are found to be associated with the similar vein systems of Aberfoyle, Storys Creek and Lutwyche located some 20 km north of Avoca. Scattered muscovite responses are also found in the western part of the Scamander field.

Gold mineralisation in North Eastern Tasmania

Northeast Tasmania is host to many Devonian lode-style gold deposits. The Tasmania Reef at Beaconsfield has a pre-mining ore reserve of about 57 000 kg of gold, about half of this now mined (Hills, 1998), making it southeastern Australia's largest single gold-producing deposit. The recent New Golden Gate discovery (located near Mathinna) by Defiance Mining contains a total resource of 212000 t @ 5.5 g/t gold (Defiance Mining NL, 2000). All of these gold deposits are found in the Cambrian to Devonian greenschist-facies turbidite rocks of the Mathinna Supergroup. The mineralisation style is generally typical of orogenic gold deposits, which are found in metamorphic terranes and which form synchronously with the late stages of orogeny (Groves *et al.* 2000).

Metamorphic terranes are also known to contain economic intrusion-related gold deposits, however in NE Tasmania the known deposits are presently uneconomic. The Fire Tower prospect in central northern Tasmania occurs in quartz stockwork veinlets in intensively sericite-carbonate altered volcanoclastic rocks of the Tyndall Group and is associated with minor sulphides. TasGold Limited has also announced promising intersections of gold mineralisation, both in the granite and country rock in the Lisle-Golconda area of northeast Tasmania. Several holes intersected extensive low-grade disseminated gold in granodiorite (to 106 m @ 0.24 g/t) at the Potoroo prospect, while high-grade gold (to 4 m @ 12.8 g/t) was intersected at the Enterprise prospect 1.5 km to the southeast (MRT 2004).

Goldfarb *et al.* (2005) describe the hydrothermal alteration associated with gold deposits in metamorphic terranes as being characteristically dominated by carbonate phases, sulphides such as pyrite and arsenopyrite and alkali metasomatism that leads to the formation of sericite, biotite, albite

and/or chlorite. This association is clearly replicated in northeast Tasmania, and it is the alkali metasomatic minerals that present the best target for ASTER mineral mapping due to their strong SWIR AIOH (kaolinite/muscovite) and Mg-FeOH/CO₃ (chlorite/epidote) absorption features. Additionally, the ASTER sensor has an excellent combination of spectral and spatial resolution at the wavelengths of these spectral features. Fe-oxide anomalies may also be expected to be associated with the oxidized zones of carbonate alteration (often found as ankerite and/or ferroan dolomite phases) and, where mineralization is outcropping, from the oxidation of auriferous pyrite and arsenopyrite.

Quartz is an almost ubiquitous component of the orogenic deposits, and five bands that comprise the ASTER TIR instrument present the opportunity to map variations in local silica content. However the TIR sensor provides data at the relatively coarse resolution of 90 m and does not distinguish between hydrothermal silica and siliceous lithologies.

Reed (2005) states that gold mineralization in northeast Tasmania exhibits characteristically narrow to non-existent alteration envelopes – a statement that is supported others as recorded in various exploration reports (e.g. Callaghan, 2004 & McClenaghan, 1994). Intrusion-related gold deposits tend to have broader alteration halos, and Callaghan (2004) describes the mineralisation within the intrusive rocks of the Lisle-Golconda mining camp as being associated with intense sericite-silica alteration with variable disseminated pyrite and arsenopyrite.

Aster responses in alteration clusters

Six (6) alteration clusters have been outlined from the interpretative layers however, other more isolated responses exist throughout the study area and might be equally significant.

Beaconsfield (Alteration Cluster 1)

Widespread silica with minor Fe-oxide, kaolinite and pyrophyllite is found closely associated with the Tasmania Reef deposit. A zone of silica & muscovite/kaolinite responses is also found 8 km to the northwest near York Town.

A small cluster of kaolinite dominated responses occur near the town of Holwell with no known occurrences associated with them. Between Winleigh and Glengary there are a number of small zones of alteration again with no known occurrences.

Lillydale (Alteration Cluster 2)

The concentration of many of the ASTER responses in the Lillydale cluster may be related to the occurrence of more intrusion-related deposits in this area. Few responses are found in the central Lisle mining camp (e.g. near Enterprise), instead the ASTER responses are found in the periphery and are associated with minor occurrences. The lack of alteration associate with this district is suspected to be due to strong vegetation masking.

Kaolinite and Fe-oxide responses exist near the Lone Star/Patersonia group of occurrences south of Lisle. The West Wiangata occurrence, some 5 km north of Golconda is coincident with strong muscovite and kaolinite response. A large pyrophyllite/silica response is found 4km NW of the Lebrina townsite. Notably, there is a discrete moderate kaolinite /sericite alteration zone mapped by ASTER associated with a small clay mine.

Various scattered silica, muscovite, alunite, kaolinite and pyrophyllite responses are also found in other areas with no known occurrence close by. Further away from Lisle, 15 km to the northwest between Retreat and Pipers Brook are a number of strong ASTER responses. Another similar zone exists near the township of Blumont, 12 km east of Lisle.

Mathinna (Alteration Cluster 3)

A north-northeast regional-scale corridor of gold mineralisation extends 90 km from Fingal to Waterhouse in northeast Tasmania. The corridor hosts a number of regularly-spaced mining camps, of which those northernmost (Lyndhurst, Forester & Warrentina and Alberton) do not appear to be associated with any ASTER responses. However from just south of Alberton and through the Dans Rivulet, Mathinna and Tower Hill mining camps is a zone of ASTER responses that follow along the trend of the regional corridor. The ASTER responses are dominated by fe-oxide, alunite & silica, with muscovite, kaolinite & pyrophyllite occurring as isolated patches.



Mt Cameron (Alteration Cluster 4)

Few ASTER anomalies occur associated the gold occurrence in the vicinity of the town of Gladstone, although, as previously mentioned in the tin discussion, 7 km to the southeast of Gladstone near South Mount Cameron there are some strong silica responses with minor alunite that are closely associated with tin mineralisation.

Whitemark (Alteration Cluster 5)

One of the best developed ASTER responses (Target 5) occurs on Flinders Island where several alluvial tin prospects were explored in the mid 1900s. Target 5 is developed over a 15 km strike length and exhibits a well-defined zonation pattern from central silica/kaolinite, through phyllic (muscovite) to propylitic assemblages (chlorite/epidote). No production is recorded and little geological information exists to describe the primary mineralization.

Cape Barren Island (Alteration Cluster 6)

This alteration cluster consists of a small number of kaolinite/alunite? alteration zones. A number of Sn occurrences (alluvial?) occur in the immediate vicinity while to the west the Mt Kerford Sn occurrence is noted.

Conclusion

The results of this investigation have provided an initial encouragement for the utility of ASTER in vegetated and weathered terrains of NE Tasmania. A large number of ASTER responses have been identified that will warrant follow-up by field workers, however the salient points resulting from this investigation are provided below.

- ASTER Mineral mapping and interpretation has been undertaken. The results have been condensed into three layers, silica responses, Fe-oxide response and SWIR. The SWIR layer includes muscovite, kaolinite, alunite, pyrophyllite, epidote and chlorite responses.
- The results are somewhat limited by vegetation, post mineral cover sequences, weathering, and the restricted nature of alteration envelopes that occur with the major deposit types.
- Six (6) broad Target areas have been identified that group together clusters of ASTER responses. Other, more isolated responses exist throughout the study area and might be equally significant.
- Some Exogranitoid deposits have silica/kaolinite/muscovite ASTER signatures. An arcuate zone of Fe-oxide, AlOH & silica ASTER anomalies extending from 4 km south to 14 km east of Pioneer warrants follow-up for Exogranitoid-type mineralization.
- A well zoned alteration pattern is exhibited by the ASTER responses that comprise the Whitemark target on Flinders Island (Target 5) where several alluvial tin prospects were explored in the 1950s and 60s. Little modern exploration data has been found to describe the primary mineralisation style(s) in this area.
- Silica, Fe-oxide, kaolinite and other minerals have been mapped in the Beaconsfield district and in the surrounding region (Target 1).
- Due to heavy vegetation, several mining camps show no ASTER responses whatsoever, including the northern and central gold districts that lie along the 90 km Fingal-Waterhouse gold mineralised corridor. Further south, the Dans Rivulet, Mathinna and Tower Hill districts are associated with Fe-oxide, alunite & silica dominated ASTER responses (Target 3).
- Several ASTER responses occur where no mineral occurrences are known.

In concluding this report, it should be stressed that the analysis approach adopted in this study aimed to derive alteration-related ASTER anomalies from the detection of strong (“deep”) absorption features by comparing all spectra in each image area. In following-up the results of this investigation workers should consider an alternative approach whereby ASTER data analysis is conducted at the mining-camp scale in order to detect and characterize more subtle spectral variations.

The ASTER responses presented could be followed up on the strength and mineral assemblage alone however Global Ore recommends that this information should be analysed using a multi-layered GIS approached with other regional geochemical, geological and geophysical datasets. This will help to properly prioritise alteration responses in the context of the integrated dataset.



10. References

- ASTER Science Project Website, 2007. Crosstalk phenomenon & correction software.
http://terrast.aster.ersdac.or.jp/en/science_info/cross.html
- Boardman JW, (1998). Leveraging the high dimensionality of AVIRIS data for improved subpixel target unmixing and rejection of false positives: Mixture tuned matched filtering (MTMF). AVIRIS 1998 Proceedings, JPL, California. 6 pp.
(http://makalu.jpl.nasa.gov/docs/workshops/98_docs/8.pdf)
- Bottrill, R. S. 1992. The Mangana mining camp and adjacent gold mining areas. Report Mineral Resources Tasmania 1992/29.
- Callaghan, T. 2004. Annual Report EL41/2002 April 2003 – April 2004. TasGold Ltd. Unpublished Mineral Resources Tasmania Report
- Defiance Mining NL. 2000. Quarterly Report to the Stock Exchange, June 2000
- Earth Observatory Website (NASA), 2007. Normalized Difference Vegetation Index (NDVI).
<http://earthobservatory.nasa.gov/Library/MeasuringVegetation/>
- Goldfarb, R.J., Baker T., Dubé, B., Groves, D.I. & Hart, C.J.R. 2005. Distribution, Character, and Genesis of Gold Deposits in Metamorphic Terranes. Economic Geology 100th Anniversary Volume, 2005
- Groves, D.I., Goldfarb, R.J., Knox-Robinson, C.M., Ojala, J., Gardoll, S., Yun, G.U., Holyland, P., 2000. Late-kinematic timing of orogenic gold deposits and significance for computer-based exploration techniques with emphasis on the Yilgarn Block, Western Australia. Ore Geology Reviews 17, 1 –38.
- Hills, P. B. 1998. Tasmania gold deposit, Beaconsfield, in: Berkman, D. A.; Mackenzie, D. H. (ed.). Geology of Australian and Papua New Guinean Mineral Deposits. 467–472. Monograph Serial Australasian Institute of Mining and Metallurgy 22.
- Johnson, B. R. and S. J. Young, 1998. "In-Scene Atmospheric Compensation: Application to SEBASS Data Collected at the ARM Site," Technical Report, Space and Environment Technology Center, The Aerospace Corporation, May 1998.
- Kalinowski & Oliver, 2004, ASTER Mineral Index Processing Manual, Remote Sensing Applications, Geoscience Australia. (http://www.ga.gov.au/image_cache/GA7833.pdf) 37 pp.
- Keele, R. A. 1994. Structure and veining in the Devonian-aged Mathinna–Alberton gold lineament, northeast Tasmania. Report Mineral Resources Tasmania 1994/06.
- MMAJ (Metal Mining Agency of Japan), 2000, Technical development report: Examination of indices for discriminating rocks and minerals and their universal validity. p. III 1-31.
- MRT 2004. Mineral exploration opportunities in Tasmania. Promotional Report on MRT Web Site: <http://www.mrt.tas.gov.au>
- Purvis, J. G. 1981. Final report on exploration at the old Royal George tin mine, EL 7/78 N.E. Tasmania. CRA Exploration Pty Ltd [TCR 81-1662].
- Reed, A. R. 2004. Gold mineralisation and regional Palaeozoic structure of the Mathinna Supergroup, eastern Tasmania. Tasmanian Geological Survey Record 2004/01.
- Ruxton, P. A. 1984. Evaluation of the Old Royal George tin mine E.L. 7/78, N.E. Tasmania. Billiton Australia [TCR 90-3149].
- Taheri, J. & Bottrill, R. S. 2005. Devonian granites and associated mineralisation in northeast and northwest Tasmania. Tasmanian Geological Survey Record 2005/03.

11. DVD DATA REFERENCE LIST

DVD 1

- Main Report and MapInfo Data
 - Maps – MapInfo files used in map creation, includes mineral maps and their interpretations
 - Report

DVD 2

- Preprocessing Raw / CrossTrack / Atmospheric Corrected
 - Raw ASTER Imagery (AST270 – AST277)
 - Cross-track illumination corrected HDF files
 - ENVI FLAASH atmospherically corrected data

DVD 3

- Preprocessing Layer Stack / MNF / Mosaics
 - ENVI Layer Stacked resampled VNIR/SWIR imagery
 - Minimum Noise Fraction transformed SWIR imagery
 - VNIR/SWIR ERMapper Mosaics

DVD4

- Processing ASTER Scenes and Mineral Maps (AST270 – AST275)
 - SWIR Mineral maps
 - TIR Silica Processing
 - VNIR Fe-oxide Ratios

DVD 5

- Processing ASTER Scenes and Mineral Maps (AST276 – AST277)
 - SWIR Mineral maps
 - TIR Silica Processing
 - VNIR Fe-oxide Ratios